processes

MDPI

Article

Extrusion Modification: Effect of Extrusion on the Functional Properties and Structure of Rice Protein

Yuxuan Gao [1,†], Yi Sun [1,†], Yu Zhang [2], Yuankuo Sun [1] and Tie Jin [1,*]

[1] Department of Food Science and Engineering, Yanbian University, Yanbian 133002, China
[2] Department of Food Science and Technology, Kongju National University, Chungnam 314701, Korea
* Correspondence: jintie@ybu.edu.cn; Tel.: +86-433-243-5577; Fax: +86-433-243-5600
† These authors contributed equally to this work.

Abstract: Modification of rice protein by extrusion technology can broaden the range of processing and applications for food and feed raw materials. In this study, rice protein was extruded at different screw speeds (100–250 rpm), extrusion temperatures (90–150 °C), and moisture contents (25–40%). Compared with an unextruded protein, the functional properties and structural properties of textured rice protein were evaluated. The results showed that, after extrusion, the solubility of protein was improved, by up to 19.76%, which was 45.23% higher than pre-extrusion; the water holding capacity of extruded rice protein was highest at 200 rpm, 130 °C, and 25%, which could be enhanced by 37.74%; the emulsion stability was enhanced by 152.82% at 200 rpm, 130 °C, and 35%. Under extrusion, the content of sulfhydryl and disulfide bonds of rice protein decreased significantly; the hydrogen bond content increased, and the ionic bond content decreased; the hydrophobic effect decrease, except at 200 rpm, 130 °C, and 40%. The microstructure changed significantly after extrusion, producing protein aggregates with a tight structure. No new characteristic peaks appeared after extrusion, but transformation occurred between the components of the secondary structure: β-sheet and β-turn angles to an α-helix structure toward the transformation, but β-sheet was still the main component. As a safe and efficient modification method, extrusion cooking can effectively improve the functional properties of rice protein to enrich the application of rice protein resources.

Keywords: rice protein; extrusion; functional properties; structural properties

Citation: Gao, Y.; Sun, Y.; Zhang, Y.; Sun, Y.; Jin, T. Extrusion Modification: Effect of Extrusion on the Functional Properties and Structure of Rice Protein. *Processes* **2022**, *10*, 1871. https://doi.org/10.3390/pr10091871

Academic Editors: Vlad Mureşan and Adriana Paucean

Received: 29 April 2022
Accepted: 16 July 2022
Published: 16 September 2022

1. Introduction

Protein is the material basis of life activities and plays an important role in regulating human physiological metabolism. At the same time, protein is also an indispensable nutrient for human life activities [1]. In the past, people mainly used animal protein as a high-quality protein source (such as meat, milk, eggs, etc.), but with the growth of population and the improvement of people's living standards, the traditional animal protein supply mode can no longer meet people's daily needs. Developing countries, in particular, are generally in a crisis of protein resource shortage. In contrast, developed countries have a large intake of animal protein leading to obesity, diabetes and other health problems [2,3]. So people have started to look for sustainable alternatives to animal protein. Many inexpensive plant proteins are good alternatives to animal proteins [4]. From an industry perspective, food manufacturers are also looking for functional plant proteins to replace animal proteins, such as proteins in food formulations, meat, and dairy proteins, because plant proteins are better for the environment and health [5].

There are many sources of plant proteins, among which, rice protein has become a recognized high-quality plant protein resource due to its low allergenicity and high digestibility, and its amino acid ratio is in line with the ideal model recommended by the World Health Organization and Food and Agriculture Organization (WHO/FAO) [6]. The processing and utilization of rice protein and the development of related nutritious and

healthy products from rice protein have also received wide attention in the food field. However, the interaction of hydrogen bonds and disulfide bonds between rice proteins makes the hydrophobic groups cross-link to form insoluble aggregates [7]. Its hydrophobic amino acid content is much higher than that of other proteins [8], which results in poor water solubility of rice proteins, and further negative effects on their functional properties. Therefore, people began to pay attention to applying reasonable modified technology to improve the functional properties of rice protein, broaden its application scope, and improve its application value.

At present, the typical food protein modification methods include physical modification, chemical modification, and enzymatic modification [9]. However, the application of chemical modification is limited by the generation of toxic effects and the toxic residue of the chemical reagent. Although there are few harmful by-products in enzymatic hydrolysis, the effect of a low degree of hydrolysis is not ideal, and a high degree of hydrolysis will produce bitter peptides, which will reduce the edible value of protein products [10]. Thus, physical modification is more reliable than chemical methods and enzymatic modification. It has a more negligible impact on the nutritional properties of the protein, and is less expensive and more conducive to large-scale industrial continuous production.

Extrusion is suitable for industrialized and continuous production, efficient and energy-saving food processing technology, and is also an excellent physical modification method. Under the synergistic action of high temperature, high pressure, and high shear in the extruder, the advanced structure of the protein will be unfolded, linearized, and re-cross-linked, resulting in the weakening of the binding force to maintain the tertiary and quaternary structures of the protein. Protein molecules are reorganized from spherical aggregation to fibrous, and the spatial conformation of the protein changes and denaturation occurs [11].The structure of the study by Yang et al. also showed that extrusion processing is an effective way to change the microstructure and digestibility of rice [12].

In order to improve the utilization value of rice protein, the extrusion method was used to modify rice protein in this experiment, and the changes in the functional properties and structure of rice protein after extrusion were explored to provide a theoretical basis for improving the development and application of rice protein.

2. Materials and Methods

2.1. Materials

Rice protein was purchased from Xi'an LvRuquan Biological Co., Ltd. (Xi'an, China), containing 91.47% and 3.84% protein, and 4.69% moisture.

2.2. Reagents

Tris-HCl, urea, H_2SO_4, 2% boric acid, EDTA, and SDS were purchased from Sigma-Aldrich Co. (St. Louis, MO, USA); other chemical reagents were purchased from Solarbio Technology Co., Ltd. (Beijing, China).

2.3. Extrusion

Rice protein was extruded by a co-rotating twin-screw extruder (DS32-III: Jinan Hisense Machinery Co., Ltd.; Jinan, China), as shown in Figure 1. The machine mainly consists of a feeding system, extrusion system, control system, and other units. The die is a circular die with a diameter of 5 mm. The length of the screw is 742 mm, and the diameter is 3.2 cm. The screw configuration is a building block structure, which is composed of a high shear kneading block with full pitch thread, 2/3 pitch thread, and 1/2 pitch thread. The barrel comprises three heating zones and is controlled by circulating cooling water. The extruder screw speed (100–250 rpm) and extrusion temperature (90–150 °C) were adjusted by a control panel. The moisture content of feed is regulated by a water pump (25–40%). As shown in Table 1, we divided the three groups of factors into four levels for the test, feed by single-screw feeder with a feed speed of 150 g/min. After the extrusions reached a stable state, the textured rice protein (TRP) was collected, and then dried at 50 °C for 8 h.

The dried TRP was stored in PVE bags until further analysis. Before analysis, TRP was ground into fine powders (screened using a 200 mesh sieve).

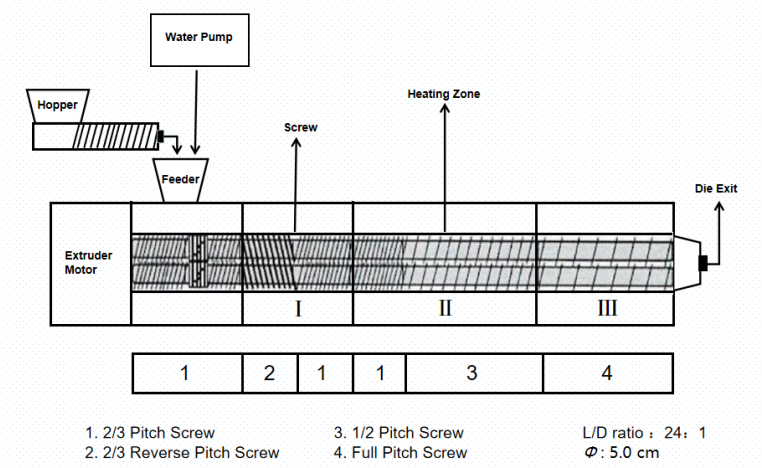

Figure 1. Twin-screw configuration and extrusion process.

Table 1. The element and corresponding level of experiment.

Level	Factors		
	Screw Speed/rpm	**Extrusion Temperature/°C**	**Moisture Content/%**
1	100	90	25
2	150	110	30
3	200	130	35
4	250	150	40

2.4. Functional Characteristics

2.4.1. Solubility

Solubility is represented by the nitrogen solubility index (NSI). A total of 200 mg of sample was dispersed in 20 mL deionized water, dissolved by magnetic stirring, and centrifuged at 4000 r/min for 20 min. The protein and total protein content of the supernatant was determined by Kjeldahl nitrogen determination and calculated according to the following Equation (1):

$$\text{NSI (\%)} = (\text{Presence of protein in supernatant}/\text{Protein content in sample}) \times 100\% \quad (1)$$

2.4.2. Water-Holding Capacity and Oil-Holding Capacity

According to the method described by Kamara et al. [13], the water-/oil-holding capacity (WHC and OHC) of the sample was determined with some modifications. A 200 mg sample was dispersed in a 15 mL centrifuge tube with 10 mL distilled water/corn oil. The precipitation quality was determined after magnetic stirring for 30 min and centrifugation at 20 °C 4000× *g* for 15 min. The calculation formula is as follows:

$$\text{WHC (mg/mg)} = (M2 - M1)/M1 \quad (2)$$

$$\text{OHC (mg/mg)} = (M2 - M1)/M1 \quad (3)$$

where M1 is the weight of sample; M2 is the weight of sediment.

2.4.3. Foaming Capacity and Stability

The sample (100 mg) was taken in a 50 mL measuring tube and dissolved in PBS buffer (20 mL, 0.01 M, pH = 7). The volume V0 was recorded. Then, the sample was dispersed by a dispersion machine (10,000 r/min) for 2 min, and the volume V1 was recorded. The

volume V2 was recorded after standing for 30 min. The following formula was used to calculate the foaming capacity and stability (FC and FS):

$$FC\ (\%) = [(V1 - V0)/V0] \times 100\% \quad (4)$$

$$FS\ (\%) = [(V2 - V0)/V0] \times 100\% \quad (5)$$

where the V0 is the volume of the initial sample, V1 is the volume of the sample after beating, and V2 is the volume after 30 min.

2.4.4. Emulsion Properties and Emulsification Stability

Determination of emulsification and emulsification stability (EAI and ESI) were determined by Singh et al. [14]. A 60 mg sample was added with 6 mL PBS buffer (0.01 M, pH = 7) and magnetically stirred at room temperature for 30 min. Then, 2 mL of corn oil was added and transferred into the centrifuge tube and then dispersed with a disperser at 20,000 r/min for 1 min. A 50 uL emulsion was quickly absorbed in the bottom and mixed with a 0.1% SDS solution (*w/v*) for 5 s. The absorbance (A0) was measured at 500 nm. After 10 min, a 50 uL emulsion was again taken from the bottom and added into 5 mL of SDS solution. After mixing, the absorbance (At) was measured at 500 nm.

$$EAI\ (m^2/g) = (2 \times 2.303 \times A0 \times N)/(C \times \varphi \times 104); \quad (6)$$

$$ESI\ (\%) = [(A0 \times t)/(A0 - At)] \times 100\% \quad (7)$$

where A0 and At represented the absorbance at 500 nm measured immediately after emulsion formation and after t (t = 10) min, respectively; C refers to the protein concentration (g/mL) before emulsification, while φ is the oil volume fraction (*v/v*) of the emulsion (φ = 0.25).

2.5. Structural Property

2.5.1. Sulfhydryl and Disulfide Bonds

When the free sulfhydryl content (SHF) was determined, according to the method of Kato and Nakai [15], a 15 mg sample was dissolved in a 5 mL Tris-Gly buffer (0.086 M Tris, 0.09 M Gly, 0.04 M EDTA, and pH = 8), then added with 50 ul of Ellman's reagent (DTNB in Tris-Gly, 4 mg/mL) reacted at 25 °C for 1 h, and the absorbance was determined at 412 nm. When total sulfhydryl (SHT) was determined, 4 mL of a 20 M Tris-Gly buffer was added into 1 mL of the protein solution, and then precipitated with 20% TCA for 1 h, centrifuged at 4000× *g* r/min for 10 min, washed with 20% TCA 3 times, and dissolved with 10 mL of Tris-Gly. A total of 200 uL of Ellman's reagent was added to 4 mL of protein solution, and the absorbance was measured at 412 nm. The contents of total sulfhydryl, free sulfhydryl, and disulfide bonds were calculated according to the following formula:

$$SH\ (umol/g) = (73.53 \times A412 \times D)/C \quad (8)$$

$$S\text{-}S\ (umol/g) = (SHT - SHF)/2 \quad (9)$$

where C is the sample concentration; D is the dilution multiple.

2.5.2. Chemical Force

The protein chemical force determination was based on the method of Tan [16] and was improved to analyze the cross-linking mode between proteins by using the difference in solubility of proteins in different extracting solutions.

Extraction solution ①: pH = 7.6 0.035 M PBS solution

Extraction solution ②: pH = 7.6 extraction solution ① + 1.5% (*m/v*) SDS solution

Leaching solution ③: pH = 7.6 leaching solution ① + 8 M urea

A total of 500 mg of the sample (dry weight) was weighed into 10 mL of ①, ② and ③ extracts, and separated and extracted (homogenized at 5000 r/min for 2 min, shaken at room temperature for 2 h, then centrifuged at 4500× *g* r/min for 20 min, filtered on

1000 mesh filter cloth) to obtain supernatants S1, S2, S3. The extraction of precipitation was repeated, and the supernatants obtained were combined by two centrifuges at 4 °C. The supernatants were then stored at 4 °C. The protein concentrations of P1, P2, and P3 were determined by the Lowery method, with P1 representing the ionic bond concentration, the difference between P2 and P1 representing the hydrophobic interaction force, and the difference between P3 and P1 representing the hydrogen bond concentration.

2.5.3. FTIR Spectroscopy

An IRTracer-100 spectrometer (Shimadzu, Kyoto, Japan) was used for FTIR spectroscopy analysis. Approximately 5 mg protein was mixed with 200 mg potassium bromide (KBr) and ground. Absorption intensity was measured at 2 cm^{-1} resolution, and the scanning wave ranged from 4000 to 400 cm^{-1}. PeakFit 4.12 software (SPSS Inc., Chicago, IL, USA) and OMNIC (Thermal, Inc., Condell Park, Australian) were used to preprocess and analyze the raw spectra.

2.5.4. Microstructure Analysis

With reference to Yang's method with slight modifications [12], after grinding, samples were placed on a specimen holder taped with double-sided Scotch tape and sputter-coated with gold, and the apparent morphology was observed using a scanning electron microscope (SEM; SU8010, Hitachi, Tokyo, Japan) at 5 kV voltage.

2.6. Statistical Analysis

Origin 8.5 (OriginLab Corporation, Northampton, MA, USA) and SPSS 17.0 (IBM Corporation, Yorktown Heights, NY, USA) analysis of variance (ANOVA) were used to plot the data and analyze the significant differences. The data were repeated 3 times in each group. The results were expressed as mean ± standard deviation.

3. Results and Discussion

3.1. Functional Characteristics

3.1.1. Solubility

The nitrogen solubility index (NSI) is one of the most important functional properties of proteins, and it is closely related to the emulsification, foaming, and gelation of proteins. During the extrusion process, the protein is modified and the NSI changes under the combined effect of temperature, shear force, and pressure.

As shown in Table 2, the NSI of TRP was improved by up to 45.23% after extrusion at 200 rpm, 150 °C, and 30%, compared to the unextruded rice protein. This may be due to the fact that, after extrusion, the molecular chain of TRP is extended, exposing the peptide bond, which facilitates hydrolysis and improves the NSI [17]. Screw speed, extrusion temperature, and moisture content all had highly significant effects on the protein NSI ($p < 0.01$).

Table 2. Functional properties of the TRP with different extrusion parameters.

Screw Speed/rpm	Extrusion Temperature/°C	Moisture Content/%	NSI/%	WHC/g·g^{-1}	OHC/g·g^{-1}	FC/%	FS/%	EAI/m^2/g	ESI/%
	Rice protein		13.62 ± 0.07 ^{hi}	2.25 ± 0.13 ^{ef}	1.55 ± 0.023 ^{abcd}	75.00 ± 0.10 ^{ab}	61.67 ± 0.13 ^{a}	20.11 ± 0.31 ^{d}	13.65 ± 0.08 ^{f}
100	130	30	17.62 ± 0.15 ^{c}	2.61 ± 0.14 ^{bcd}	1.52 ± 0.060 ^{cd}	63.33 ± 0.06 ^{cd}	10.96 ± 0.06 ^{ef}	18.77 ± 0.19 ^{e}	17.88 ± 0.08 ^{e}
150	130	30	16.61 ± 0.04 ^{e}	2.86 ± 0.26 ^{abc}	1.54 ± 0.01 ^{bcd}	55.71 ± 0.04 ^{de}	17.62 ± 0.016 ^{cd}	20.40 ± 0.12 ^{d}	23.51 ± 0.21 ^{c}
200	130	30	16.41 ± 0.15 ^{e}	2.59 ± 0.05 ^{cd}	1.56 ± 0.09 ^{abcd}	67.48 ± 0.04 ^{bc}	11.37 ± 0.02 ^{de}	18.47 ± 0.19 ^{e}	20.96 ± 0.26 ^{d}
250	130	30	14.12 ± 0.15 ^{g}	2.16 ± 0.28 ^{e}	1.59 ± 0.04 ^{abcd}	80.72 ± 0.07 ^{a}	13.25 ± 0.08 ^{cde}	17.71 ± 0.09 ^{f}	20.51 ± 2.13 ^{d}
200	90	30	18.75 ± 0.09 ^{b}	2.88 ± 0.01 ^{ab}	1.61 ± 0.11 ^{abc}	54.71 ± 0.00 ^{ef}	26.06 ± 0.02 ^{b}	25.79 ± 0.18 ^{a}	14.85 ± 0.72 ^{f}
200	110	30	16.22 ± 0.12 ^{ef}	2.47 ± 0.14 ^{de}	1.58 ± 0.02 ^{abcd}	67.48 ± 0.02 ^{ab}	7.65 ± 0.01 ^{e}	13.63 ± 0.27 ^{h}	22.79 ± 0.25 ^{c}
200	130	30	16.41 ± 0.15 ^{e}	2.59 ± 0.05 ^{cd}	1.56 ± 0.09 ^{abcd}	67.48 ± 0.04 ^{bc}	11.37 ± 0.02 ^{de}	18.47 ± 0.19 ^{e}	20.96 ± 0.26 ^{d}
200	150	30	19.78 ± 0.10 ^{a}	2.60 ± 0.11 ^{cd}	1.49 ± 0.04 ^{d}	72.654 ± 0.01 ^{abc}	7.07 ± 0.01 ^{e}	24.82 ± 0.34 ^{b}	20.96 ± 0.26 ^{d}
200	130	25	17.36 ± 0.09 ^{d}	3.10 ± 0.01 ^{a}	1.50 ± 0.05 ^{d}	47.67 ± 0.01 ^{f}	25.33 ± 0.02 ^{bc}	22.21 ± 0.06 ^{c}	20.52 ± 0.17 ^{d}
200	130	30	16.41 ± 0.15 ^{e}	2.59 ± 0.05 ^{cd}	1.56 ± 0.09 ^{abcd}	67.48 ± 0.04 ^{bc}	11.37 ± 0.02 ^{de}	18.47 ± 0.19 ^{e}	20.96 ± 0.26 ^{d}
200	130	35	13.83 ± 0.06 ^{h}	2.99 ± 0.13 ^{a}	1.64 ± 0.03 ^{a}	67.48 ± 0.02 ^{bc}	19.95 ± 0.01 ^{bc}	17.75 ± 0.13 ^{f}	34.50 ± 0.12 ^{a}
200	130	40	10.34 ± 0.08 ^{k}	2.85 ± 0.02 ^{abc}	1.62 ± 0.05 ^{ab}	74.87 ± 0.02 ^{ab}	55.17 ± 0.02 ^{a}	14.87 ± 0.14 ^{g}	32.82 ± 0.66 ^{b}

Different letters (a, b, c, d, e, f, g, h, i) in the same column indicate a significant difference ($p < 0.05$).

With the increase in screw speed, the shear strength in the extruder increases. Under the action of shear force, the molecular space structure increases, making the water molecules easy to penetrate, which is conducive to the degradation of large molecules. At the same time, due to the stirring effect of the screw, water is uniformly dispersed in the material. However, if the speed is too high, the NSI will start to decrease due to the shortening of the action time of the material in the extruder and the incomplete fragmentation and degradation of the macromolecular material.

At the beginning of extrusion, the NSI increases with the decrease in extrusion temperature and reaches a minimum at 110 °C. This may be due to the fact that when the temperature started to warm up, the molecular structure of some proteins was broken and some small molecules were dissolved out [18], which decreased the NSI of TRP. When the temperature was higher than 110 °C, the NSI increased significantly.

With the increase in moisture content, the NSI of TRP showed a decreasing trend. Water in the extruder is equivalent to lubricant. Thus, when the moisture content of the material continues to increase, it will lead to the formation of a synergistic effect between the disulfide bond and hydrogen bond, disulfide bond and the hydrophobic interaction in protein, and the elongation of protein [18].

3.1.2. WHC and OHC

A good WHC and OHC, which can increase the juicy performance of food, reduces processing loss and food's greasy feeling, and makes food have a good taste. As shown in Table 3, extrusion temperature, moisture content, and screw speed significantly affected the WHC of TRP ($p < 0.05$). Compared to unextruded rice protein, the WHC of TRP was increased, and the highest increase was by 37.74% at 200 rpm, 130 °C, and 25%. The reason for this phenomenon may be that the ability of the protein to interact with water is enhanced after extrusion [19]. WHC first increased and then decreased with the increase in screw speed.

Table 3. One-way ANVOA analysis of the functional properties of textured rice protein.

Extrusion Parameters		NSI	WHC	OHC	FC	FS	EAI	ESI
Screw speed/rpm	F	1055.66	7.59	0.050	321.12	12.19	29.30	7.31
	P	4.41×10^{-13} ***	0.004 **	0.994	1.64×10^{-10} ***	0.010 *	0.002 ***	0.011 *
Extrusion temperature/°C	F	1507.19	1507.19	1.419	83.35	10.29	49.91	1.58
	P	7.46×10^{-14} ***	7.46×10^{-14} ***	0.297	1.22×10^{-7} ***	0.01 *	0.001 ***	0.27
Moisture content/%	F	2522.62	47.71	3.235	161.34	15.70	7.39	9.11
	P	5.70×10^{-15} ***	1.76×10^{-6} ***	0.060	4.89×10^{-9} ***	0.001 ***	0.011 *	0.005 **

* Significant at $p < 0.05$; ** Significant at $p < 0.01$; *** Significant at $p < 0.001$. F: the significance of the entire fitted equation. P: the degree of non-rejection of the original hypothesis.

With the increase in screw speed and shear force, the dense spatial structure of the protein molecule was destroyed, resulting in the decrease in the molecular weight of the polypeptide chain, the increase in the number of polar groups and the surface area of the material, the looser structure of the protein, the increase in the adsorption capacity, and the better combination with water. However, when the screw speed increased to a certain extent, the protein structure received a greater change in shear force. Higher screw speed resulted in a reduction in the retention time, resulting in the material not being fully restructured in the cavity, and the pressure generated by the extrusion on the die head was also reduced accordingly [19]. Therefore, when the melt left the cavity of the extruder, the expansion degree decreased, and the structure was dense. Thus, the WHC of the sample was reduced. WHC increased with the increase in extrusion temperature, indicating that extrusion had an impact on the protein structure. This change caused TRP to obtain a better WHC. With the increase in temperature, the binding degree of water to protein was also higher. Moisture content also affected the WHC due to the effect of water in the extrusion process, which increases the molecular motility of polymer chain segments, increases elasticity, and reduces torque and mechanical energy consumption. Therefore,

when the moisture content increases, the degree of swelling of protein molecules and the ability to form molecular networks increases [20].

As shown in Table 3, extrusion temperature and moisture content, and screw speed had no significant effect on the OHC of TRP ($p > 0.05$), which is consistent with the conclusion obtained by Mazaheri Tehrani et al. [19]. The OHC was increased after extrusion, but the increase was not significant. The increase in OHC may be due to the cracking of the chemical bonds of the polymeric substances during the extrusion process, causing a change in molecular polarity, while the high pressure destroyed the external state and the internal molecular structure of the material, forming a porous structure [21].

3.1.3. FC and FS

Extrusion temperature, moisture content and screw speed had significant effects ($p < 0.05$) on the FC and FS of TRP (Table 3). The FC of TRP was improved compared to that of unextruded rice protein. At 250 rpm, 130 °C, and 30%, the FC was 80.72%, which was 7.62% higher compared to pre-extrusion (Table 2). The FS of TRP decreased significantly and was the lowest at 200 rpm, 150 °C, and 30%, at only 7.07%, which was 88.54% lower compared to the pre-extrusion period. Since the basic unit of foam is a bubble surrounded by a liquid film, factors affecting the protein FC and FS include the diffusivity of protein molecules, the magnitude of interfacial tension, and the distribution of hydrophobic groups. The reason for the decrease in FS in this paper may be due to the fact that the disulfide bonds that maintain the higher structure of the protein are broken by shear and friction after rice protein extrusion, which makes the protein less able to maintain surface tension at the gas–liquid interface and reduces the strength of the gas–liquid film, making the bubble easy to rupture.

3.1.4. EAI and ESI

Emulsification of proteins is one of the important functional properties of proteins and is often used in meat, dairy, beverage, and pasta products to improve the sensory and physicochemical properties of the products. Proteins can reduce the surface tension at the oi–water interface and promote the formation of oil–water emulsions. In addition, proteins adsorb and unfold on the surface of emulsified oil droplets to form a protective film that prevents oil droplets from aggregating and maintains the emulsified state [22].

Extrusion temperature, moisture content, and screw speed significantly affected the EAI and ESI of TRP ($p < 0.05$). Extrusion can contribute to increasing the ESI for textured proteins under different conditions. At 200 rpm, 130 °C, and 25%, the ESI could reach 34.50%, an increase of 152.82% compared to rice protein. The EAI of TRP ranged from 14.87 to 25.79 m^2/g.

Hydrophobicity and NSI were the main determinants of emulsification activity [23]. The high temperature and shear forces induced by the extrusion process can change the distribution pattern of hydrophilic and hydrophobic sites on the protein surface, resulting in some degree of disruption of the protein structure. During this period, changes in the state of existence of disulfide bonds and aggregation, and depolymerization of protein particles may occur (as shown by the results of the structural property), and their secondary bonds can be opened, exposing the functional groups of the protein, thus affecting protein hydrophobicity and leading to changes in ESI. Fischer [24] also explored the effects of extrusion temperature (110, 130, 160 °C) and moisture content (18%, 25%) on the structural and emulsification properties of soy protein concentrate. The emulsification activity increased by approximately 1.6 times at a 25% moisture content of protein, and increased with increasing temperature, where the temperature reached a maximum at 160 °C with an increase of about 2.2-fold. This finding is similar to the present study. Thus, proper denaturation of proteins usually increases their surface activity [25], which contributes to their adsorption at the oil–water interface and to the formation of physical layers, thus enhancing the ESI.

3.2. Structural Property

3.2.1. Sulfhydryl and Disulfide Bonds

Extrusion breaks chemical bonds and interactions between protein molecules and/or other molecules and turns the plant protein into a textured plant protein meat analogue by forming new chemical cross-links. In addition, the interactions between disulfide bonds and non-covalent bonds are the main forces that maintain the structure. The study of changes in the content of SHF and disulfide bonds is an important way to explore the role of disulfide bonds. It was found that extrusion has an effect on sulfhydryl and disulfide bonds of TRP. After extrusion treatment, the content of both sulfhydryl and disulfide bonds decreased significantly (Table 4). SHT decreased from 19.70 μmol/mg to 4.86 μmol/mg, a decrease of 75.33%. SHF decreased from 6.01 μmol/mg to 0.93 μmol/mg, a decrease of 84.53%, and disulfide bonds decreased from 6.84 μmol/mg to 1.72 μmol/mg, a decrease of 74.85%.

Table 4. One-way ANOVA analysis of the molecular structure of textured rice protein.

Extrusion Parameters		SHT	SHF	S-S [1]	Ionic Bonds	Hydrogen Bonds	Hydrophobic Interaction
Screw speed/rpm	F	2231.81	240.22	321.12	7.17	4.71	2.62
	P	1.05×10^{-14} ***	6.89×10^{-10} ***	3.98×10^{-14} **	0.012 *	0.035 *	0.123
Extrusion temperature/°C	F	1834.87	204.85	1025.31	1.93	7.73	10.54
	P	2.79×10^{-14} ***	1.5×10^{-9} ***	5.09×10^{-13} ***	0.203	0.011 *	0.004 **
Moisture content/%	F	314.94	204.61	140.95	48.05	5.70	8.42
	P	1.80×10^{-10} ***	1.52×10^{-9} ***	9.50×10^{-9} ***	0.001 ***	0.022 *	0.007 **

* Significant at $p < 0.05$; ** Significant at $p < 0.01$; *** Significant at $p < 0.001$; [1] Disulfide bonds. F: the significance of the entire fitted equation. P: the degree of non-rejection of the original hypothesis.

During the extrusion, shear is an important factor affecting the SHF and disulfide bond content. Mechanical shear breaks the disulfide bonds between protein molecules by virtue of physical shear, reducing the content of disulfide bonds. For example, Fischer [24] found that SHF in extruded wheat protein decreased from 20.54×10^{-9} qmol/mg to 8.68×10^{-9} qmol/mg under shear. Burgess and Stanley [26] determined the SHF and disulfide bond content of extruded soybean protein and also found that the extruded soybean protein disulfide bonds decreased from 4.5×10^{-8} mol/mg to 0.9×10^{-8} moL/mg after extrusion. Therefore, we believe that extrusion can severely disrupt the formation of disulfide bonds.

When the moisture content gradually increased from 25% to 40%, the SHT of TRP showed a complex trend of decreasing, then increasing, and then decreasing again, and the trend of disulfide bonds was similar. Moisture content significantly affected the sulfhydryl and disulfide bonds of proteins ($p < 0.05$), but there was no pattern of change. The reason for the complex changes in disulfide bonds may be due to reduction/oxidation or free radical reactions between disulfide bonds and sulfhydryl groups in the presence of the water [17,25]. During extrusion, conversion between disulfide bonds and SHT and SHF occurs. However, under high temperature and shear, sulfur-containing amino acids or the sulfhydryl groups within them may also decompose, and the destruction after extrusion is greater than the reorganization of sulfhydryl groups, which leads to the reduction in SHT in the sample. Similarly, extrusion temperature is an important factor affecting the content of sulfhydryl and disulfide bonds, and extrusion temperature has a significant negative effect on the SHF of TRP, which decreases with increasing temperature [27]. Furthermore, the content of SHT and disulfide bonds decreased and then increased with extrusion temperature; when the extrusion treatment was higher than 110 °C, the content of disulfide bonds increased from 1.72 μmol/mg to 2.04 μmol/mg.

3.2.2. Chemical Force

Ionic and hydrogen bonds, which are weaker bonding forces relative to non-disulfide covalent and disulfide bonds, are important forces in maintaining the conformation of protein molecules, and they are mainly found between polar groups of protein molecules [28].

Compared to rice proteins, there was a decreasing trend in the ionic bonding content of TRP after extrusion treatment (Table 5). The greatest decrease was observed at 200 rpm, 130 °C, and 30%, with a decrease of 5.6%. Moreover, with the increase in screw speed, extrusion temperature, and moisture content, the ionic bond content showed a decreasing trend, and the hydrogen bond content hydrophobic interaction showed an increasing trend. After extrusion, the hydrogen bonding content of TRP was elevated in comparison to rice protein. The greatest increase was observed at 200 rpm, 130 °C, and 40%, which could be elevated by 19.83%. This may be related to the fact that protein molecules will form hydrogen bonds with other protein molecules more easily in the hydrophobic microenvironment of the protein. This is also supported by the result that the relative content of protein hydrophobic groups increases at 200 rpm, 130 °C, and 40%. The relative content of hydrogen bonds tends to decrease with increasing screw speed and extrusion temperature. Since ionic and hydrogen bonds are weaker bonding forces compared to non-disulfide covalent and disulfide bonds, the hydrogen and ionic bonds that maintain the protein conformation are broken under the effect of heat and the disruptive effect of high pressure and high shear force.

Table 5. Structural properties of TRP with different extrusion parameters.

Screw Speed/rpm	Extrusion Temperature/°C	Moisture Content/%	SHT/μmol·g^{-1}	SHF/μmol·g^{-1}	S-S[1]/μmol·g^{-1}	Ionic Bonds/mol·g^{-1}	Hydrogen Bonds/mol·g^{-1}	Hydrophobic Interaction/mol·g^{-1}
	Rice protein		19.70 ± 0.48 ^{a}	6.01 ± 0.52 ^{a}	6.84 ± 0.15 ^{b}	1159.00 ± 0.00 a	2611.80 ± 38.03 b	2809.16 ± 12.27 ab
100	130	30	4.92 ± 0.07 ^{d}	1.19 ± 0.05 ^{de}	1.86 ± 0.03 ^{cd}	1139.22 ± 28.41 bc	2915.39 ± 10.41 ab	2706.66 ± 38.95 cb
150	130	30	5.48 ± 0.12 ^{cd}	1.21 ± 0.11 ^{de}	2.14 ± 0.10 ^{cd}	1142.41 ± 3.41 abc	2814.3 ± 40.51 ab	2714.07 ± 12.36 cb
200	130	30	5.07 ± 0.15 ^{d}	1.22 ± 0.03 ^{de}	1.93 ± 0.07 ^{cd}	1094.00 ± 11.82 e	2726.81 ± 17.82 ab	2755.80 ± 38.21 abc
250	130	30	5.01 ± 0.13 ^{d}	1.16 ± 0.01 ^{de}	1.92 ± 0.06 ^{cd}	1133.71 ± 727 ^{bc}	2651.03 ± 20.12 ^{b}	2679.03 ± 18.36 ^{c}
200	90	30	5.56 ± 0.17 ^{cd}	1.67 ± 0.08 ^{bc}	1.94 ± 0.12 ^{cd}	1122.64 ± 7.27 ^{cd}	2886.16 ± 41.27 ^{ab}	2698.44 ± 37.36 ^{cb}
200	110	30	4.86 ± 0.07 ^{d}	1.42 ± 0.22 ^{cd}	1.72 ± 0.12 ^{d}	1120.36 ± 1.36 ^{cd}	2818.44 ± 0.64 ^{ab}	2784.39 ± 1.41 ^{abc}
200	130	30	5.07 ± 0.15 ^{d}	1.22 ± 0.03 ^{de}	1.93 ± 0.07 ^{cd}	1094.00 ± 11.82 e	2726.81 ± 17.82 ab	2755.80 ± 38.21 abc
200	150	30	5.02 ± 0.25 ^{d}	0.93 ± 0.02 ^{e}	2.04 ± 0.12 ^{cd}	1100.14 ± 32.95 ^{de}	2641.66 ± 14.05 ^{b}	2676.30 ± 45.50
200	130	25	6.77 ± 1.20 ^{b}	1.85 ± 0.07 ^{b}	2.46 ± 0.64 ^{b}	1135.36 ± 0.91 ^{abc}	2810.44 ± 39.91 ^{ab}	2706.66 ± 38.95 ^{cb}
200	130	30	5.07 ± 0.15 ^{d}	1.22 ± 0.03 ^{de}	1.93 ± 0.07 ^{cd}	1094.00 ± 11.82 e	2726.81 ± 17.82 ab	2755.80 ± 38.21 abc
200	130	35	6.20 ± 0.41 ^{bc}	1.72 ± 0.08 ^{bc}	2.24 ± 0.18 ^{bc}	1150.14 ± 0.23 ^{ab}	2963.66 ± 45.23 ^{ab}	2676.30 ± 45.50 ^{c}
200	130	40	5.11 ± 0.03 ^{d}	1.09 ± 0.15 ^{de}	2.01 ± 0.08 ^{cd}	1121.73 ± 1.36 ^{cd}	3129.07 ± 18.36 ^{a}	2855.57 ± 15.59 ^{a}

Different letters (a, b, c, d, e) in the same column indicate a significant difference ($p < 0.05$).

Compare to rice protein, the hydrophobic effect of TRP decreased, except at 200 rpm, 130 °C, and 40%. Rice proteins in their natural state mostly exist in the form of globular protein bodies with hydrophobic residues inside, and a large molecular weight aggregate is formed between proteins through hydrophobic interaction. After extrusion of rice protein, the hydrophobic residues of protein were destroyed, the hydrophobic interaction was reduced, and the protein was dispersed, leading to an increase in soluble protein content. The hydrophobic effect of TRP increased with the increase in moisture content and was higher than that of rice protein at 40% moisture content, which may as a result of the increase in moisture content facilitating the unfolding of protein structure and promoting the exposure of hydrophobic groups. This may be due to the denaturation of the protein at the beginning of the heat treatment, which exposed the hydrophobic groups and contributed to the relative enhancement of hydrophobic interactions [29].

3.2.3. FTIR Spectroscopy

Protein secondary structure refers to the regularly repeated conformation in the protein polypeptide chain, which is maintained by hydrogen bonds formed between the carbonyl and amide groups in the backbone. The secondary structures are mainly α-helix, β-sheet, β-turn, and random coil. Exploring the changes in the secondary structure of rice protein under different extrusion processes can reflect, to some extent, the effect of different treatments on the protein structure.

The FTIR spectra of the rice proteins are shown in Figure 2. The S1 region (3600–2750 cm^{-1}) contains the vibrational absorption peaks of hydroxyl (-OH), amino (-NH), methyl (-CH3), and methylene (-CH2). The S2 region (1750–1250 cm^{-1}) is mainly the amide vibrational region and the mixed region of a protein, fatty acid, and polysaccharide. The S3 region (1250–930 cm^{-1}) is the characteristic absorption region of polysaccharide. The peaks in the S3 re-

gion (1250–930 cm^{-1}) are characteristic of polysaccharides, while the S4 region (930–500 cm^{-1}) is weak, but several small peaks are present, making it a fingerprint region. The range of maximum absorption peak wave numbers was essentially the same for the TRP compared to the rice protein; the characteristic absorption peak positions and characteristic fingerprints are the same, and the baseline trend is the same, but there is a great difference in the absorption intensity at the same peak position. This indicates that the chemical composition is essentially unchanged, with slight differences in vibrational intensities. Extrusion resulted in the changes in the chemical bonds and forces between the molecules, thus altering the spatial structure of the protein. Characteristic absorption peaks were present in the S2 region, but there was no significant difference between the characteristic absorption peaks of rice protein and TRP, and no new absorption peaks were formed. Therefore, no new amide bonds (i.e., peptide bonds) were generated in the protein after extrusion.

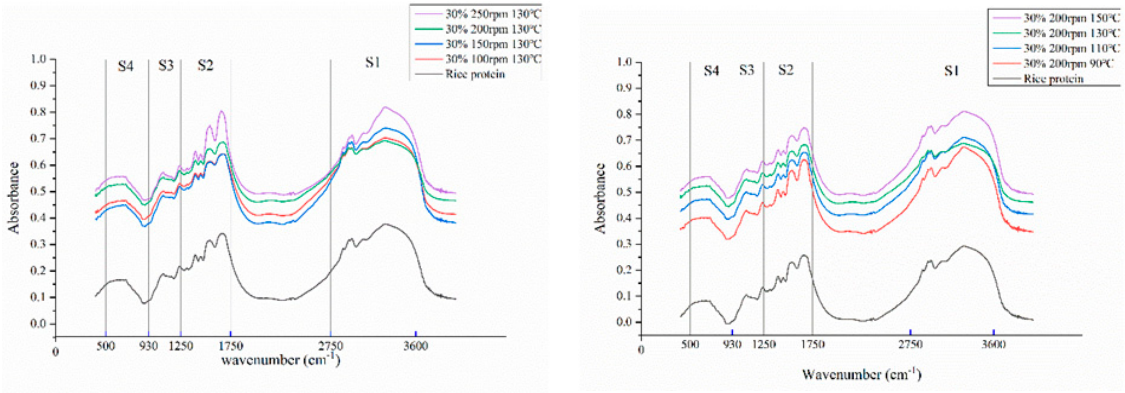

(**a**) (**b**)

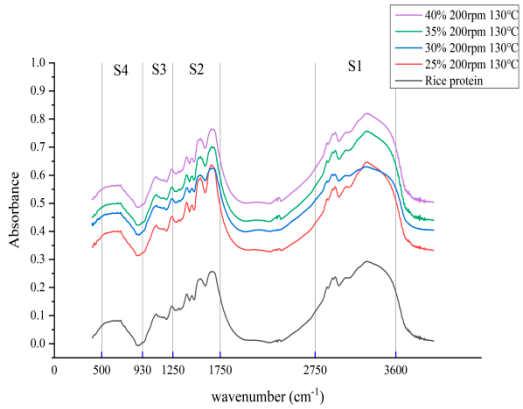

(**c**)

Figure 2. FITR spectrum of TRP with different extrusion parameters (**a**) FITR spectrum of TRP at different screw speeds; (**b**) FITR spectrum of TRP at different extrusion temperatures; (**c**) FITR spectrum of TRP at different moisture contents.

In the amide I region of the protein (1600–1700 cm^{-1}), the secondary structure information of the protein can usually be obtained by deconvoluted peak shape fitting. The correspondence between the individual sub-peaks and the secondary structure after spectral peak fitting was carried out with reference to the method of Petruccelli and Añón [29]. The results are shown in Table 6. The results showed that whether before or after extrusion, β-sheet was the major structure that accounted for the largest proportion of the protein secondary structure. When the moisture content was increased from 25% to 30%, the β-sheet of TRP increased from 38.96% to 44.33%, while the α-helix of TRP decreased from 26.47% to 23.04%. The extrusion temperature also affected the secondary structure of the

protein. When the extrusion temperature was raised from 90 °C to 130 °C, the β-sheet and β-turn content of TRP gradually increased, and the α-helix content gradually decreased; however, when the temperature was raised to 150 °C, the β-sheet and β-turn content decreased, and the ordered structure decreased (Table 6). Prudêncio et al. [30] analyzed the infrared spectra of soybean isolate extrudates at different temperatures (140, 160, 180 °C) and moisture contents (30% and 40%) and found similar results. The changes in the protein secondary structure were influenced by the extrusion temperature, and TRP did not completely linearize or transform into α-helix and random coil, still retaining a certain amount of ordered structure (β-sheet and β-turn). At temperatures above a certain threshold, the ordered secondary structure of the protein begins to be completely lost. The level of this threshold varies considerably depending on the extruded raw material.

Table 6. Protein secondary structure of TRP under different extrusion parameters.

Screw Speed/rpm	Extrusion Temperature/°C	Moisture Content/%	α-Helix/%	β-Sheet/%	β-Turn/%
	Rice protein		24.93 ± 1.30^{abc}	43.99 ± 1.43^{ab}	31.08 ± 0.20^{bcd}
100	130	30	21.74 ± 3.66^{c}	41.78 ± 0.72^{ab}	36.50 ± 3.07^{a}
150	130	30	24.77 ± 2.32^{abc}	43.06 ± 3.82^{ab}	32.17 ± 1.51^{bcd}
200	130	30	23.04 ± 1.58^{bc}	44.33 ± 5.15^{ab}	32.63 ± 4.01^{bcd}
250	130	30	27.73 ± 3.29^{a}	42.94 ± 3.17^{ab}	29.33 ± 0.25^{d}
200	90	30	25.94 ± 1.73^{ab}	42.50 ± 3.13^{ab}	31.56 ± 1.42^{bcd}
200	110	30	24.09 ± 0.87^{abc}	45.84 ± 0.82^{a}	30.08 ± 0.24^{cd}
200	130	30	25.04 ± 1.68^{abc}	44.33 ± 5.15^{ab}	32.03 ± 4.01^{bcd}
200	150	30	25.84 ± 2.08^{ab}	40.68 ± 3.99^{ab}	33.48 ± 1.92^{abc}
200	130	25	26.47 ± 2.26^{ab}	38.96 ± 5.44^{b}	34.57 ± 3.18^{ab}
200	130	30	23.04 ± 1.58^{bc}	44.33 ± 4.17^{ab}	33.23 ± 3.11^{bcd}
200	130	35	24.94 ± 0.55^{abc}	42.62 ± 2.18^{ab}	32.44 ± 1.63^{bcd}
200	130	40	26.08 ± 0.32^{ab}	40.86 ± 2.09^{ab}	33.06 ± 1.79^{abcd}

Different letters (a, b, c, d) in the same column indicate a significant difference ($p < 0.05$).

3.2.4. Microstructure Analysis

The microstructure of the proteins under different extrusion conditions still differed significantly. The microstructure of the rice protein showed a smooth and regular spherical structure. The diameter of the rice protein aggregates was small (50–500 um), and the proteins were more dispersed. The protein aggregates showed a spherical shape, with varying sizes, a very smooth surface, and a uniform distribution, with clear boundaries between the protein aggregates (Figure 3A,B).

The shape of the TRP at 200 rpm, 90 °C, and 30% was in between other TRPs. Under a high magnification lens, the rough surface of the protein, and the delaminated and wrinkled epidermis were observed. The smooth spherical structure was disrupted and a gluten network-like structure with air cells was present. The air cells were more than the TRP at 200 rpm, 130 °C, and 30%, and the structure was looser, with unclear edges and a tendency to melt.

With TRP at 200 rpm, 130 °C, and 30%, the roughest surface can be observed at 5 K magnification. The scanned image at high magnification showed that the surface of the protein structure becomes loose, with an increased surface area and the presence of air cells, which are uneven in size, layered, and interwoven in a network. The size of the air cells is not uniform, but the air cells are tightly arranged. This also indicates that the RPI was degraded and polymerized to varying degrees during the extrusion, and its naturally ordered structure was broken, with protein molecules degrading and polymerizing each other to form a lamellar structure.

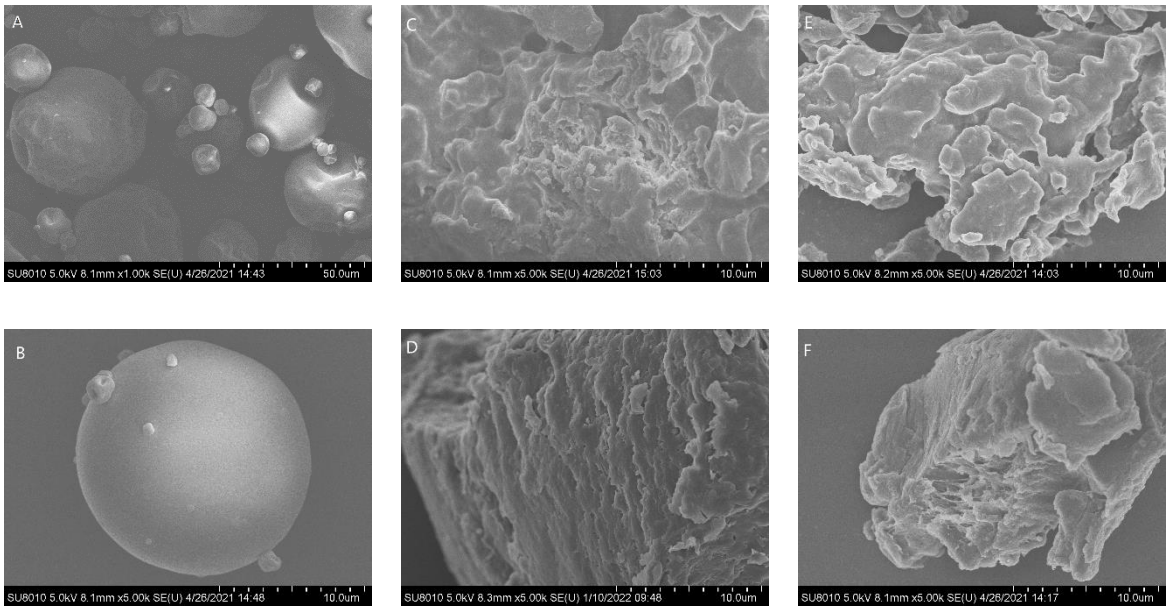

Figure 3. SEM micrographs of the textured rice protein at different extrusion parameters (**A**) Rice protein at 1 K magnification; (**B**) Rice protein at 5 K magnification; (**C**) TRP at 5 K magnification at 200 rpm, 90 °C, and 30%; (**D**) TRP at 5 K magnification at 200 rpm, 130 °C, and 30%; (**E**) TRP at 5 K magnification at 100 rpm, 130 °C, and 30%; (**F**) TRP at 5 K magnification at 200 rpm, 130 °C, and 40%.

In contrast, TRPI at 200 rpm, 130 °C, and 40% was observed under 5 K magnification. The surface of the protein was febrile and dense, with a regular linear texture in the same direction. There was a regular laminar distribution. Moisture content can be considered as a key factor affecting the level of TRP tissue organization. In the presence of free water, the forces between the screw and the material, and between the barrel wall and the material cause the protein network to elongate and thin, Tearing and perforation occur when this stretching exceeds a certain threshold, resulting in the destruction of the network and the appearance of a fiber-like flocculent structure. When there is enough moisture, it is less likely to stretch and perforate under the action of moisture tension, and the protein structure with high moisture is more compact and less porous. With TRP at 100 rpm, 130 °C, and 30% at 5 K magnification, it is observed that the surface is rough, the structure is looser, the edges of the lamellae are not well defined, and the melting tendency is more pronounced compared to a 200 rpm screw speed.

4. Conclusions

In conclusion, extrusion has an effect on both the functional and structural properties of rice protein. During extrusion, the extrusion parameters (screw speed, extrusion temperature, and moisture content) significantly affected the functional properties of the proteins such as WHC, FC, FS, ESI, and EAI ($p < 0.05$). After extrusion, the WHC of TRP was highest at 200 rpm, 130 °C, and 25%, which could be enhanced by 37.74% compared to unextruded protein; FC was 80.72% at 250 rpm, 130 °C, and 30%, an enhancement of 7.62%; EAI was highest at 34.50% at 200 rpm, 130 °C, and 35%, an enhancement of 152.82%. The improvement of the functional properties of rice protein can facilitate more applications of rice protein in food. For example, after upgrading the WHC and NSI, rice protein can be used in products such as juice and sports drinks to increase the nutritional content of the products; after upgrading the FC and FS, rice protein can be used as a food additive—foaming agent; and after upgrading the EAI, rice protein can be used in ice cream, desserts and prepared foods. By improving the functional properties of rice protein through extrusion, it can meet a variety of consumer needs.

Under extrusion, the SHT of rice protein decreased from 19.70 μmol/mg to 4.86 μmol/mg and SHF decreased from 6.01 μmol/mg to 0.93 μmol/mg. The disulfide bonds decreased from

6.84 μmol/mg to 1.72 μmol/mg, hydrogen bond content increased, ionic bonds decreased, and hydrophobic interactions decreased, except for at 200 rpm, 130 °C, and 40%. The secondary structure of the protein was not completely linearized after extrusion, and still retained an amount of ordered structure (β-sheet and β-turn), and β-sheet was the main component (more than 40%). No new absorption peaks appeared in the FTIR infrared spectrum, and no new amide bonds (i.e., peptide bonds) were generated. The change in the protein structure by extrusion is the reason for the change in the functional properties of the protein.

Author Contributions: Conceptualization, Y.G. and T.J.; validation, Y.G. and Y.S. (Yi Sun); for-mal analysis, Y.G. and Y.Z.; investigation, Y.S. (Yi Sun) and Y.S. (Yuankuo Sun); resources, T.J.; writing—original draft preparation, Y.G. and Y.Z.; writing—review and editing, Y.G. and Y.Z.; visualization, Y.G. and T.J.; supervision, T.J.; funding acquisition, T.J. All authors have read and agreed to the published version of the manuscript.

Funding: This research received no external funding.

Institutional Review Board Statement: Not applicable.

Informed Consent Statement: Not applicable.

Data Availability Statement: Data are contained within the article.

Acknowledgments: Thank you to Korea Kongju University for providing the laboratory for this study.

Conflicts of Interest: The authors declare no conflict of interest. The funders had no role in the design of the study; in the collection, analyses or interpretation of data; in the writing of the manuscript or in the decision to publish the results.

References

1. Zayas, J.F. *Functionality of Proteins in Food*; Springer: Cham, Switzerland, 1997.
2. Moorthi, R.N.; Vorland, C.J.; Gallant, K.M.H. Diet and Diabetic Kidney Disease: Plant Versus Animal Protein. *Curr. Diabetes Rep.* **2017**, *17*, 1–8.
3. Zhong, V.W.; Allen, N.B.; Greenland, P.; Carnethon, M.R.; Ning, H.; Wilkins, J.T.; Lloyd-Jones, D.M.; van Horn, L. Protein Foods from Animal Sources, Incident Cardiovascular Disease and All-Cause Mortality: A Substitution Analysis. *Int. J. Epidemiol.* **2021**, *50*, 223–233. [CrossRef] [PubMed]
4. Hertzler, S.R.; Lieblein-Boff, J.C.; Weiler, M.; Allgeier, C. Plant Proteins: Assessing Their Nutritional Quality and Effects on Health and Physical Function. *Nutrients* **2020**, *12*, 3704. [CrossRef] [PubMed]
5. Sha, L.; Xiong, Y.L. Plant Protein-Based Alternatives of Reconstructed Meat: Science, Technology, and Challenges. *Trends Food Sci. Technol.* **2020**, *102*, 51–61. [CrossRef]
6. Samard, S.; Gu, B.Y.; Ryu, G.H. Effects of Extrusion Types, Screw Speed and Addition of Wheat Gluten on Physicochemical Characteristics and Cooking Stability of Meat Analogues. *J. Sci. Food Agric.* **2019**, *99*, 4922–4931. [CrossRef]
7. Van Der Borght, A.; Vandeputte, G.E.; Derycke, V.; Brijs, K.; Daenen, G.; Delcour, J.A. Extractability and Chromatographic Separation of Rice Endosperm Proteins. *J. Cereal Sci.* **2006**, *44*, 68–74. [CrossRef]
8. Yadav, R.B.; Yadav, B.S.; Chaudhary, D. Extraction, Characterization and Utilization of Rice Bran Protein Concentrate for Biscuit Making. *Br. Food J.* **2011**, *113*, 1173–1182. [CrossRef]
9. Keenan, E.K.; Zachman, D.K.; Hirschey, M.D. Discovering the Landscape of Protein Modifications. *Mol. Cell* **2021**, *81*, 1868–1878. [CrossRef]
10. Carr, J.W.; Loughheed, T.C.; Baker, B.E. Studies on Protein Hydrolysis. IV.—Further Observations on the Taste of Enzymic Protein Hydrolysates. *J. Sci. Food Agric.* **1956**, *7*, 629–637. [CrossRef]
11. Samard, S.; Ryu, G.H. A Comparison of Physicochemical Characteristics, Texture, and Structure of Meat Analogue and Meats. *J. Sci. Food Agric.* **2019**, *99*, 2708–2715. [CrossRef]
12. Yang, W.; Zheng, Y.; Sun, W.; Chen, S.; Liu, D.; Zhang, H.; Fang, H.; Tian, J.; Ye, X. Effect of Extrusion Processing on the Microstructure and in Vitro Digestibility of Broken Rice. *LWT* **2020**, *119*, 108835. [CrossRef]
13. Kamara, M.T.; Amadou, I.; Tarawalie, F.; Huiming, Z. Effect of Enzymatic Hydrolysis on the Functional Properties of Foxtail Millet (*Setaria italica* L.) Proteins. *Int. J. Food Sci. Technol.* **2010**, *45*, 1175–1183. [CrossRef]
14. Singh, A.; Sharma, S.; Singh, B. Effect of Germination Time and Temperature on the Functionality and Protein Solubility of Sorghum Flour. *J. Cereal Sci.* **2017**, *76*, 131–139. [CrossRef]
15. Kato, A.; Nakai, S. Hydrophobicity Determined by a Fluorescence Probe Method and Its Correlation with Surface Properties of Proteins. *Biochim. Biophys. Acta* **1980**, *624*, 13–20. [CrossRef]
16. Tan, F.J.; Lai, K.M.; Hsu, K.C. A comparative study on physical properties and chemical interactions of gels from tilapia meat pastes induced by heat and pressure. *J. Texture Stud.* **2010**, *41*, 153–170. [CrossRef]

17. Fang, Y.; Zhang, B.; Wei, Y. Effects of the Specific Mechanical Energy on the Physicochemical Properties of Texturized Soy Protein during High-Moisture Extrusion Cooking. *J. Food Eng.* **2014**, *121*, 32–38. [CrossRef]
18. Shih, M.C.; Kuo, C.C.; Chiang, W. Effects of Drying and Extrusion on Colour, Chemical Composition, Antioxidant Activities and Mitogenic Response of Spleen Lymphocytes of Sweet Potatoes. *Food Chem.* **2009**, *117*, 114–121. [CrossRef]
19. Maurya, A.K.; Said, P.P. Extrusion Processing on Physical and Chemical Properties of Protein Rich Products-An Overview. *J. Bioresour. Eng. Technol.* **2014**, *2*, 61–67.
20. Xu, E.; Wu, Z.; Pan, X.; Long, J.; Wang, F.; Xu, X.; Jin, Z.; Jiao, A. Effect of Enzymatic (Thermostable α-Amylase) Treatment on the Physicochemical and Antioxidant Properties of Extruded Rice Incorporated with Soybean Flour. *Food Chem.* **2016**, *197*, 114–123. [CrossRef]
21. Wittek, P.; Zeiler, N.; Karbstein, H.P.; Azad Emin, M. High Moisture Extrusion of Soy Protein: Investigations on the Formation of Anisotropic Product Structure. *Foods* **2021**, *10*, 102. [CrossRef]
22. Lin, S.; Huff, H.E.; Hsieh, F. Extrusion Process Parameters, Sensory Characteristics, and Structural Properties of a High Moisture Soy Protein Meat Analog. *J. Food Sci.* **2002**, *67*, 1066–1072. [CrossRef]
23. Chen, L.; Chen, J.; Ren, J.; Zhao, M. Modifications of Soy Protein Isolates Using Combined Extrusion Pre-Treatment and Controlled Enzymatic Hydrolysis for Improved Emulsifying Properties. *Food Hydrocoll.* **2011**, *25*, 887–897. [CrossRef]
24. Fischer, T. Effect of Extrusion Cooking on Protein Modification in Wheat Flour. *Eur. Food Res. Technol.* **2004**, *218*, 128–132. [CrossRef]
25. Bueno, A.S.; Pereira, C.M.; Menegassi, B.; Arêas, J.A.G.; Castro, I.A. Effect of Extrusion on the Emulsifying Properties of Soybean Proteins and Pectin Mixtures Modelled by Response Surface Methodology. *J. Food Eng.* **2009**, *90*, 504–510. [CrossRef]
26. Burgess, L.; Stanley, D. A Possible Mechanism for Thermal Texturization of Soybean Protein. *Can. Inst. Food Sci. Technol. J.* **1976**, *9*, 228–231. [CrossRef]
27. Qi, P.X.; Onwulata, C.I. Physical Properties, Molecular Structures, and Protein Quality of Texturized Whey Protein Isolate: Effect of Extrusion Temperature. *J. Agric. Food Chem.* **2011**, *59*, 4668–4675. [CrossRef]
28. Naumann, S.; Schweiggert-Weisz, U.; Martin, A.; Schuster, M.; Eisner, P. Effects of Extrusion Processing on the Physiochemical and Functional Properties of Lupin Kernel Fibre. *Food Hydrocoll.* **2021**, *111*, 106222. [CrossRef]
29. Petruccelli, S.; Añón, M.C. Relationship between the Method of Obtention and the Structural and Functional Properties of Soy Protein Isolates. 1. Structural and Hydration Properties. *J. Agric. Food Chem.* **1994**, *42*, 2161–2169. [CrossRef]
30. Prudêncio-Ferreira, S.H.; Arêas, J.G. Protein-Protein Interactions in the Extrusion of Soya at Various Temperatures and Moisture Contents. *J. Food Sci.* **1993**, *58*, 378–381. [CrossRef]